ELSEVIER

Journal of Power Sources 113 (2003) 179–183

JOURNAL OF POWER SOURCES

www.elsevier.com/locate/jpowsour

Short communication

Lithium-free transition metal phosphate cathode for Li secondary batteries

M. Manickam*

Department of Electrical Engineering, Nagaoka University of Technology, 1603-1 Kamitomioka, Nagaoka, Niigata 940-2188, Japan

Received 28 August 2002; accepted 3 September 2002

Abstract

Li atoms can be inserted electrochemically into the vacant sites in the host framework structure of hexagonal $Cr_{0.5}Nb_{1.5}(PO_4)_3$ (an analog of Nasicon). Intercalation of lithium into this compound is achieved electrochemically at room temperature. The compound, $Cr_{0.5}Nb_{1.5}(PO_4)_3$, is used as a cathode of a secondary battery without any lithium initially present in the starting material. The performance of this material is discussed in view of its discharge. XRD, SEM and ESCA spectral studies are carried out on electrode surfaces before and after the insertion/extraction reactions and the results are presented.

Keywords: Lithium insertion; Vacant site; NZP; Surface analysis; Battery

1. Introduction

Secondary lithium batteries using lithium intercalation compounds as the cathode and lithium metal as the anode have been studied intensively this last decade. The cathode of a secondary lithium battery is a host compound into/from which the working Li^+ ion of the electrolyte can be inserted/extracted reversibly as a guest species over a large solubility range. However, it has been demonstrated that this type of battery (lithium metal as anode) is unlikely to reach commercialization because of safety problems. To solve this problem, a safe approach to rechargeable lithium batteries is to replace lithium metal with a lithium intercalation compound, hence referred to as a lithium-ion battery [1,2]. This was developed by Sony Energetic Inc., in 1990 [3]. The cathode materials suitable for Li-ion batteries are layered compounds are $LiCoO_2$ [3], $LiNiO_2$ [4], and $LiNi_{1-y}Co_yO_2$ [5]. Considering the high cost of Co and Ni, recently, the three-dimensional $LiMn_2O_4$ spinel phase has also been studied extensively as a cathode for Li-ion batteries. However, the cathode material must be such that it is easy to intercalate and de-intercalate lithium ions during the discharge and charge processes. This limits the use of layered and spinel structures as cathode material:

1. The removal of Li from the layered $Li_{1-x}MO_2$ oxides renders them unstable at larger x relative to the displacement of M cations to the Li layers [5].
2. On the other hand, the spinel framework has no degrees of freedom for opening the interstitial space of the closely packed oxide ion array in which Li^+ ions move, so the $Li_{1+x}[Mn_2]O_4$ cathode is limited to low-power applications [6].

Therefore, there is a motivation to identify an alternative framework host having a somewhat open interstitial space and, at the same time, an appropriate voltage using an inexpensive and environmentally friendly transition metal. Host are that has recently been explored NASICON-type compounds, many of which are good ionic conductors. Many have been found to have potential applications as cathode materials, because their crystal structures have a three-dimensional framework that allows Li ions to diffuse easily [7]. In this regard, Yoshida et al. [7] recently investigated the use of lithium transition metal phosphate as a cathode material. In this study, we explored NZP ($NaZr_2P_3O_{12}$) phases with a general formula $A^{1+}M_2^{4+}P_3O_{12}$ possessing a hexagonal symmetry for the potential use as a cathode material without any lithium present in the A-site initially. The NZP structure is versatile in that chemical substitution by a variety of elements,

* Tel.: +81-258-47-3548; fax: +81-258-47-3548.
E-mail address: lithiumbattery@hotmail.com (M. Manickam).

0378-7753/02/$ – see front matter
PII: S0378-7753(02)00476-7

is possible at Na, Zr and P sites giving rise to an isostructural phase, including a vacancy at the A-site, and leading to the formation of $Cr_{0.5}Nb_{1.5}(PO_4)_3$, transition metal phosphate, without any lithium initially. In this work, we show that Li has been inserted electrochemically into the vacant A-site in the NZP phase at room temperature [8]. Understanding the structure and composition of this material upon lithium insertion is important in view of its potential application as a battery electrode for the development of rechargeable Li batteries. This compound may be used as a cathode for a secondary battery, without containing any lithium in its structure, and this may be considered to environmentally friendly and safer than the lithium containing counterparts. The objective of this work is to elucidate the transition metal phosphate as a cathode for lithium secondary batteries and its role during discharge and charge processes. Preliminary results of characterization, including cycling life, SEM as well as XPS measurements, are presented.

2. Experimental

The transition metal phosphate $Cr_{0.5}Nb_{1.5}(PO_4)_3$ was prepared by solid-state reaction in air. Starting materials were Cr_2O_3 (99.9%), Nb_2O_5 (99.9%) and $NH_4H_2PO_4$ powder. The stoichiometric mixture was mixed thoroughly in a mortar and heated at 200 °C for 12 h to drive off NH_3, H_2O and other gaseous products. The mixture was then heated at 600 °C for 5 h and at 930 °C for 12 h with intermittent grinding. Phase identification and evaluation of lattice parameters of the product were carried out by powder X-ray diffraction (XRD) using Cu Kα radiation. Electrochemical performance was evaluated with cylindrical test cells. The procedures for the fabrication and the measurement of lithium rechargeable cells are almost the same as those described elsewhere [8]. The electrode active materials were mixed with 15 wt.% of acetylene black and with 10 wt.% of PVDF, and then pressed (wt.%: weight percent). The mixture was ground and then pressed into a disk with a diameter of 10 mm at 78 MPa. The thickness of each disk was 1 mm and the weight was about 60 mg. Each disk was dried at 80 °C for 30 min. An electrochemical testing cell was constructed with the disk as the cathode, the lithium foil as the anode, and filter paper as the separator. The electrolyte was 1 M $LiClO_4$ in EC/PC, 3:1 vol. (Tomiyama Chemicals; EC: ethylene carbonate, PC: propylene carbonate). Cell performance was evaluated galvanostatically at a current density of 0.25 mA/cm^2 with the aid of charge–discharge unit (Hokuto Denko HJ-201B). The cells were first discharged and then charged at constant current density between the potential limit of 1.5 V for discharge and 3.2 V for charge. All electrochemical measurements were carried out in a glove box filled with argon at room temperature. X-ray photoelectron spectroscopy (JEOL, JPS-9000 SX, Shimadzu) using Mg Kα radiation was used to analyze the chemical binding energy of the sample. We have used a 285.0 eV value for the C 1s signal of hydrocarbons for charge referencing spectra. The surface of the electrodes was observed with a scanning electron microscope (JEOL - T220A, Nihon Denshi).

3. Results and discussion

The X-ray diffraction pattern of $Cr_{0.5}Nb_{1.5}(PO_4)_3$ prepared by solid-state reaction in air at 930 °C is shown in Fig. 1a. The lattice parameters of the compound matched with those of the hexagonally structured $TiNb(PO_4)_3$ powder diffraction file (JCPDS) 25-0984. The data reveal that the sample is a multiphase compound with chromium phosphate and niobium phosphate as impurities. Unless the preparation temperatures are optimized, impurity phases are always formed. Although the compound is a multiphase one, interestingly, the intercalation still occurs and shows high discharge capacity as shown in this paper. The phases are stable on exposure to air and moisture at room temperature. Long-term exposure, however, leads to surface oxidation and hence the compounds are stored in a desicator. The electrochemical behavior of the sample that is exposed moisture shows a capacity loss of 25%; however, the structure remains unaltered.

Fig. 2 shows the variation of the cell voltage versus composition and capacity during the first discharge–charge cycle for a cell using $Cr_{0.5}Nb_{1.5}(PO_4)_3$ as starting material. The insertion of lithium into the $(PO_4)_3$ framework in the discharge process has two separate intercalation plateau-like regions at 2.3 and 1.6 V for $0 \leq x \leq 1$ and $1 \leq x \leq 2.3$, respectively. Using the cathode material $Cr_{0.5}Nb_{1.5}(PO_4)_3$, 2.3 Li ions per formula unit were inserted and 1.8 Li ions were extracted while at discharge and charge in the range of 3.2–1.5 V. The shape of the discharge curve Fig. 2 is characterized by an immediate sharp drop in voltage to 2.5 V, followed by a gradual downward sloping potential over a long period of x value ($x = 1$) until 2.1 V. Then, again,

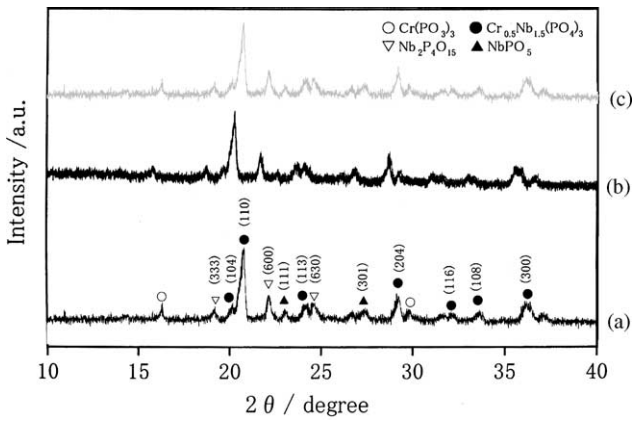

Fig. 1. X-ray diffraction patterns of $Cr_{0.5}Nb_{1.5}(PO_4)_3$ (a) before Li insertion, (b) upon Li insertion (first discharge), and (c) upon Li extraction (first charge).

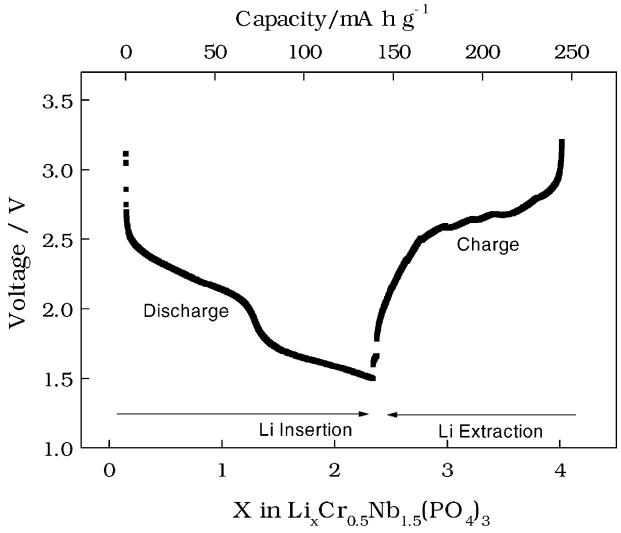

Fig. 2. Discharge and charge curves of NZP-type $Cr_{0.5}Nb_{1.5}(PO_4)_3$ cathode (without containing any lithium as starting material). Discharge: intercalation of lithium in $Cr_{0.5}Nb_{1.5}(PO_4)_3$, charge: de-intercalation from $Li_xCr_{0.5}Nb_{1.5}(PO_4)_3$. For free energy of intercalation, see text.

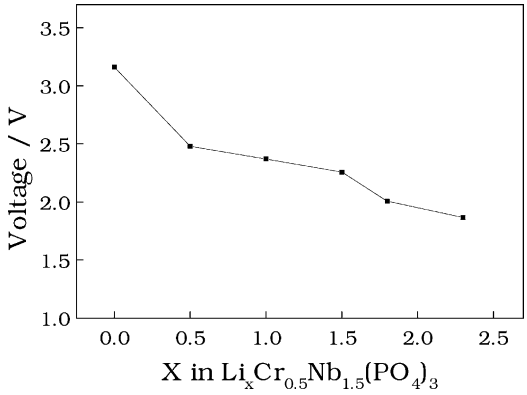

Fig. 3. Compositional variation of OCV during the first discharge of $Cr_{0.5}Nb_{1.5}(PO_4)_3$.

with a sharp drop occurs at 2 V, followed by a gradual change in voltage till 1.5 V. The initially high and rapidly falling voltage to 2.5 V indicates a high value of the Li chemical potential and its sharp decrease after occupancy of the first sites. The single-phase behavior typical of solid-state formation (voltage decreasing with x) is visible throughout the entire discharge process. The 2.1 V region corresponds to the $Nb^{5+}/^{4+}$ redox couple. On the other hand, the 1.6 V region of discharge corresponds to the $Nb^{4+}/^{3+}$ redox couple. The electrochemical capacity of this cathode $Cr_{0.5}Nb_{1.5}(PO_4)_3$ is found to be 142 mAh/g between 3.2 and 1.5 V voltage range at the current density 0.25 mA/cm^2. The mid-discharge voltage at 2.3 V and the high x value ($x = 2.3$) observed are the two phenomena that allow the calculation of a large free energy of intercalation, ΔG, for the entire process. In the discharge curve of Fig. 2, 2.3 Li atoms have been inserted at the lower cut-off limit of 1.5 V; hence, ΔG is equal to -122 kcal/mol. For comparison, ΔG for Li_xTiS_2 is -57.4 kcal/mol [9] and that for $Li_{1+x}V_3O_8$, is -200 kcal/mol [10].

To understand the intermediate intercalation process, electrochemical cycling with relaxation periods was performed. The open-circuit voltage curve of an electrochemical cell provides information of the behavior of the cell under the condition of zero current flow. The open-circuit voltage of the Li|$Cr_{0.5}Nb_{1.5}(PO_4)_3$ cell for $0 \leq x \leq 2.3$ as a function of x in the Fig. 3 was measured as follows: the cell was first discharged to a desired x ($x = 0.2$) and then left on open circuit (zero current flow) for 2 h. The final cell voltage was recorded as the open-circuit voltage for that composition. Theoretically, after the relaxation step, the cell voltage had to reach the original open-circuit voltage value [11]. The observed discrepancy in the electrochemical behavior is due to the short relaxation time especially at the lower cut-off voltage, indicating a low intercalation speed. The X-ray diffraction patterns in Fig. 1b and c were obtained following Li^+ insertion and extraction, respectively. The X-ray diffraction pattern of the lithiated compound (Fig. 1b) supports the contention that electrochemical lithiation is involved during the intercalation process. The X-ray diffraction pattern after lithiation is very similar to that initially observed before lithiation except for a limited structure expansion that is revealed by the shift of the peaks to smaller angles. The parent phase $h\ k\ l$ reflections are retained for all the samples (before Li insertion, after Li insertion/extraction), indicating that hexagonal symmetry is retained. In NZP and related phases, the 3D-linked interstitial space is occupied by alkali A ions [12]. The interstitial space contains two different sites for A ions: type I sites situated between two ZrO_6 octahedra along the c-axis with a distorted octahedral coordination, and type II sites located between endless columns with a trigonal prismatic coordination [13]. In NZP and related phases the type I sites are either partially or completely filled and the type II sites are empty. From Table 1, it is understood that the lattice parameter along the a-axis increases upon lithium insertion and decreases upon extraction. This is expected if Li-ions occupy type II sites [13]. Moreover, the lattice parameter along the c-axis decreases upon lithium insertion and increases upon extraction, which may be due to the size of the transition metal ion $Nb^{5+}/^{4+}$ upon reduction (while discharging) and $Nb^{4+}/^{5+}$ upon oxidation (while charging), respectively. Hence, the c-axis is influenced by the size of the cation at a type I site and the a-axis depends on the Li content at a type II site. Indeed, the X-ray diffraction

Table 1
Variation of lattice parameters upon lithium insertion/extraction into/from NZP-type compounds

$Li_xCr_{0.5}Nb_{1.5}(PO_4)_3$	Lattice parameter	
	a-axis (nm)	c-axis (nm)
Before lithium insertion ($x = 0$)	0.857	2.166
Upon lithium insertion ($x = 2.3$)	0.876	2.051
Upon lithium extraction ($x = 1.8$)	0.861	2.158

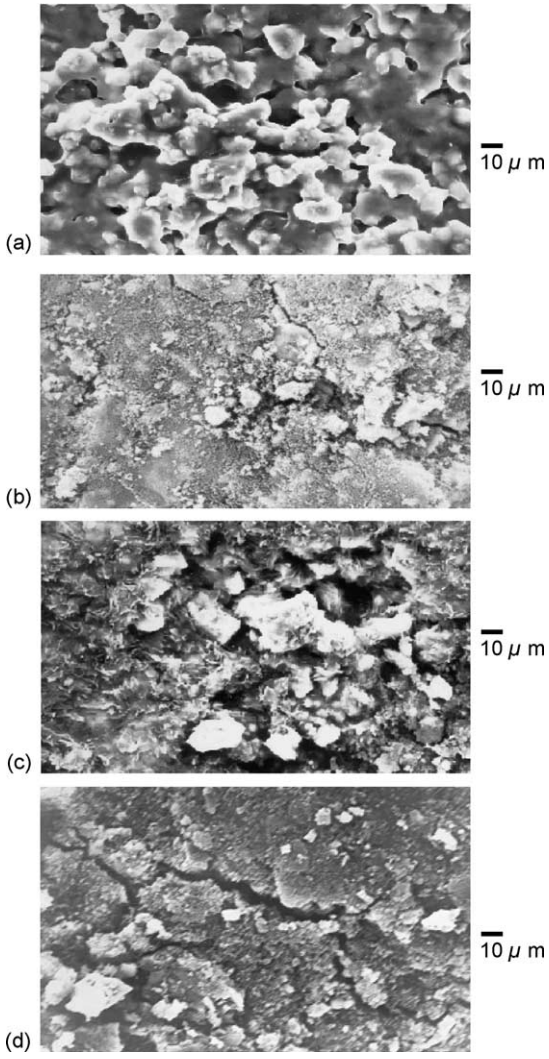

Fig. 4. Scanning electron micrographs of $Cr_{0.5}Nb_{1.5}(PO_4)_3$ cathode (a) as-sintered, (b) cathode + AB + binder: pressed under 78 MPa, (c) upon Li insertion (first discharge), and (d) upon Li extraction (first charge).

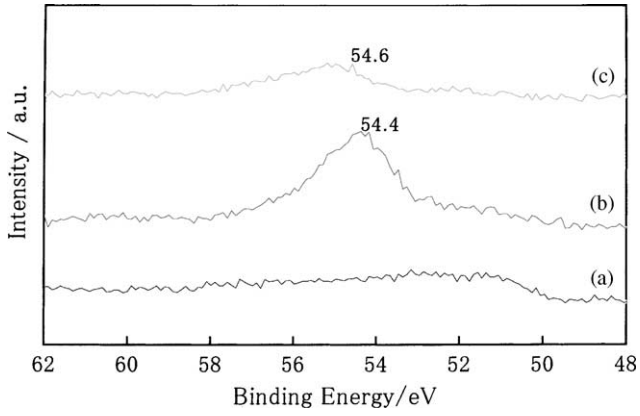

Fig. 5. ESCA spectra of Li 1s for the electrode (a) before cycling, (b) upon lithium insertion, and (c) upon extraction. The binding energy of each peak is indicated.

pattern obtained after charging, Fig. 1c, is very similar to that of the uncycled cathode, except for a peak shift that does not retained to its initial value.

3.1. SEM/ESCA studies of electrode surfaces

The morphology of as-sintered, pressed and electrochemically Li inserted/extracted samples has been studied by SEM. Examination of the surface of $Cr_{0.5}Nb_{1.5}(PO_4)_3$ by SEM revealed that the particle size is of the order of 10 μm Fig. 4a. On pressing, the particle size of the uncycled cathode reduced to 2–4 μm Fig. 4b. Upon discharge, the micrograph shows a different morphology on the electrode surface layer Fig. 4c. A white fluffy material is observed on the surface. The charged electrode surface in, Fig. 4d has a different morphology and the fluffy material on the charged surface is less than that on the discharged sample surface; this leads us to suggest that the white fluffy material may correspond to a lithium compound. In order to identify the white fluffy material, the composition of the surface layer was also studied by ESCA. After electrochemical lithium insertion, the electrode was washed with PC and dried then it was transported into the vacuum chamber of ESCA. ESCA spectra for the Li 1s electrode surface under various conditions are shown in Fig. 5. Peaks were assigned with reference to literature [14,15]. The spectrum in Fig. 5a is that of the cathode $Cr_{0.5}Nb_{1.5}$ $(PO_4)_3$, transition metal phosphate before undergoing any cyclic measurement. It can be seen from the spectrum that no peak is observed around 54.4 eV that corresponds to Li 1s. Though the sample does not contain any lithium initially, it is in agreement with the spectra. Upon discharge (insertion of lithium into the cathode), the Li 1s peak in Fig. 5b, which is attributed to Li compound, was observed. Upon charge (extraction of lithium from the cathode), the Li 1s peak at 54.6 eV (Fig. 5c), shows a decrease in relative intensity compared to discharge one. This indicates that insertion/extraction of lithium into/from the host compound influences the intensity of the Li 1s peak. Hence, careful analysis of the binding energies of the observed peak confirms that the white fluffy material observed in SEM corresponds to a lithium compound.

3.2. Cycling behavior

Fig. 6 shows the cycling behavior of the Li|$Cr_{0.5}Nb_{1.5}(PO_4)_3$ cell over a given number of cycles. The curves were recorded with a current of 0.2 mA in the range 3.2–1.5 V. There is a sharp fall in capacity for the first 5 cycles; initial capacity of 142 mAh/g decreases to 117 mAh/g, reflecting a 16% loss. Then, the cyclability improved. After 20 cycles, the cell showed almost constant capacity. From the above observation, we conclude that the Li|$Cr_{0.5}Nb_{1.5}(PO_4)_3$, secondary cell, is a technically attractive candidate for long cycle life battery applications. However, because of the low cycling voltage range (3.2–1.5 V versus 3.5–4.5 V for other systems), the

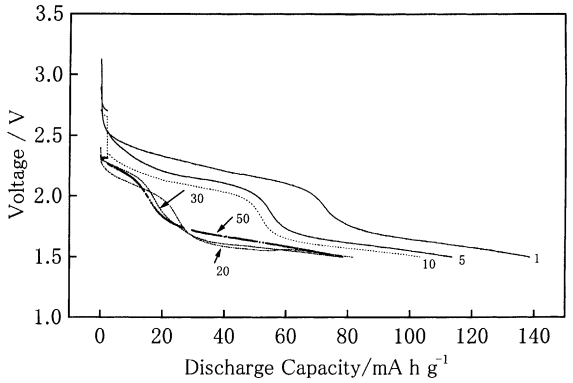

Fig. 6. Cycling behavior of Li|$Cr_{0.5}Nb_{1.5}(PO_4)_3$ cells over subsequent cycles (cycle numbers are indicated in the figure) against metallic lithium anode.

energy density of this system will be lower than that of high-voltage systems.

4. Conclusion

Our investigation of the transition metal phosphate, $Cr_{0.5}Nb_{1.5}(PO_4)_3$, reveals that the host framework is convenient for metal atom (lithium) insertion/extraction. Thus, it is confirmed that the transition metal phosphate without lithium initially can act as a cathode of appropriate voltage, reasonable energy and good reversibility in non-aqueous Li cells. Li^+ insertion at a cut-off voltage of 1.5 V is reversible, as shown by the cycling behavior and the X-ray diffraction patterns. The hexagonal symmetry is retained upon lithium insertion/extraction into/from the host material. A white fluffy material is observed on the surface of the electrodeposited Li of the cathode material, indicating the presence of a lithium compound. The ESCA spectra confirm that the white fluffy material corresponds to a lithium compound. This solid-state cathode material satisfies the basic requirements such as a large free energy of reaction $\Delta G = -122$ kcal/mol (exhibits a mid-discharge voltage of 2.3 V), and a wide composition range ($x = 2.3$) with a cut-off voltage of 1.5 V resulting in high cell discharge capacity of 142 mAh/g, and making it suitable for cycling without much structural change upon lithium insertion/extraction. Our work suggests that a transition metal phosphate is a technically attractive candidate for long cycle-life battery applications. Furthermore, this material is considered to be environmentally friendly and safe to handle, since lithium is only held as the host material.

References

[1] D.W. Murphy, J.N. Carides, J. Electrochem. Soc. 126 (1979) 349.
[2] M. Lazzari, B. Scrosati, J. Electrochem. Soc. 127 (1980) 773.
[3] K. Ozawa, Solid State Ion. 69 (1994) 212.
[4] J.R. Dahn, U. von Sacken, M.W. Juzkow, H. Al-Janaby, J. Electrochem. Soc. 138 (1991) 2207.
[5] R.J. Gummow, M.M. Thackeray, J. Electrochem. Soc. 140 (1993) 3365.
[6] M.M. Thackeray, J.O. Thomas, M.S. Whittingham, MRS Bull. 25 (2000) 39.
[7] K. Yoshida, K. Toda, K. Uematsu, M. Sato, Key Eng. Mater. 157/158 (1999) 289.
[8] M. Manickam, K. Ishibashi, M. Takata, Proc. Electrochem. Soc. Jpn. 1 (1998);
M. Manickam, M. Takata, J. Power Sources, 2002, in press.
[9] A.S. Nagelberg, W.L. Worell, J. Solid State Chem. 29 (1979) 345.
[10] G. Pistoia, M. Pasquali, M. Tocci, R.V. Moshtev, V. Manev, J. Electrochem. Soc. 133 (1985) 281.
[11] C. Delmas, F. Cherkaoui, A. Nadiri, P. Hagenmuller, Mat. Res. Bull. 22 (1987) 631.
[12] G.V. Subba Rao, U.V. Vardaraju, K.A. Thomas, B. Sivasankar, J. Solid State Chem. 70 (1987) 101.
[13] C. Delmas, R. Olazcuaga, G. Le Flem, P. Hagenmuller, F. Cherkaui, R. Brochu, Mat. Res. Bull. 16 (1981) 285.
[14] K. Kanamura, H. Tamura, S. Shiraishi, Z. Takehara, Electrochim. Acta 40 (1995) 913.
[15] B. Vincent Crist, Handbook of the Elements and Native Oxides, XPS International Inc., Kawasaki, Japan, 1999.